AIMS Energy, 9(4): 714–726.
DOI: 10.3934/energy.2021033
Received: 24 February 2021
Accepted: 01 June 2021
Published: 11 June 2021

http://www.aimspress.com/journal/energy

Research article

Optimization of the perfect absorber for solar energy harvesting based on the cone-like nanostructures

Zhaolong Wang*, Guihui Duan and Huigao Duan

National Research Center for High-Efficiency Grinding, College of Mechanical and Vehicle Engineering, Hunan University, Changsha 410082, PR China

*** Correspondence:** Email: zhaolongwang@hnu.edu.cn; Tel: +86-13548713101.

Abstract: The effects of materials, geometric parameters, and morphologies on the absorption properties of absorbers with the cone-like nanostructures surrounded by water have been numerically studied. The underlying mechanisms of the perfect absorption of solar energy are revealed by gradient index effect with electric field distributions. It shows that the absorber achieves perfect absorption for solar energy harvesting with nanocones made of Chromium (Cr), Nickel (Ni), Platinum (Pt), Titanium (Ti), and Bismuth Telluride (Bi_2Te_3), while the perfect absorption wavelength region of absorbers with nanocones made of noble metals (Au, Ag) is 300 nm to around 650 nm, which is far narrower than the solar spectrum. In addition, geometric parameters of the nanocones on the surface of the metamaterials make a big difference on the absorption properties of them though there is a small tolerance. Besides, the morphology of the cone makes a little difference on the absorption properties of the absorber, and the absorptance of the absorber increases with the increase of the number of nanocone's sides. Furthermore, the solar absorber with nanocones is sensitive to the incident angle of the light with a small tolerance, but the polarization of the incident light almost makes no difference on the absorption property of the absorber with nanocones.

Keywords: absorber; FDTD method; nanocones; optimization; solar energy harvesting

1. Introduction

Solar energy is infinite green energy on earth, which has been widely used via photo-thermal conversion, photochemical reaction, photosynthesis, as well as photo-electricity all over the world [1–4]. In the past decades, solar water heater, solar cell, photodetector, sensor, et al. have been investigated

deeply, and such kinds of equipment have been widely used [4–8]. Because of the well development of nano-fabrication techniques in the past 20 years, some enhanced applications of solar energy have been proposed, such as electricity generation enabled by solar vapor generation [9], steam sterilization [10], thermophotovoltaic (TPV) cell [11], biomimetic design [12], desalination [13–15], and so on. However, most of the solar energy is reflected, transmitted, and scattered. Therefore, the low efficiency of solar energy harvesting severely limits the further development of solar energy applications [10]. Thus, how to enhance the conversion of solar energy is in urgent need, which is attracting more and more interests in the past decades [16–19].

In the past two decades, optical absorbers with perfect light absorption property have been widely studied by researchers considering both of the materials and structures with the development of the nano-optics theory. For the narrow band absorption enhancement, some specially designed nanostructures made of noble metallic materials, such as gold (Au), silver (Ag), aluminum (Al), exhibit enhanced light absorption property because of the plasmon resonance aroused by certain light wave [20–23]. Then, the light will be converted into other kinds of energy (heat, electricity, et al.) due to ohmic loss or dielectric loss [24–27]. Furthermore, some metal oxide-based semiconductor materials are also used in absorbers for photo-thermal conversion, such as Ti_2O_3, TiO_2, and Fe_3O_4 [28–30]. Those semiconductors generate electron-hole pairs and relax to band edges when they expose to solar light. As for the broad spectrum absorption enhancement [30,31], carbonaceous materials and polymers with black color demonstrate excellent broadband light absorption properties. Under the irradiation of an external light source, the lattice vibration of these materials contributes to the photo-thermal conversion. However, their instability and toxic feature severely limit their widely applications in reality [32].

Recently, the sub-wavelength metamaterials have received more and more attentions because of their unique properties which are merely found in nature [33,34]. Metamaterial is an artificial material to achieve special light manipulation, such as negative refractive index material and photonic crystal at the beginning [35]. Metamaterials have also been employed for the broadband absorption of light by combining different materials and specially designed structures [19,36–39]. For example, Au nanoparticles work with Al_2O_3 porous medium achieve quite broadband absorption [40], while absorbers with nano-pyramids made of hyperbolic materials, such as hBN and Bi_2Te_3 [38,41], also demonstrate broadband absorption properties because of the numerous inside plasmon resonances instead of the surface plasmon resonance of metamaterials made of noble metals [42]. In addition, the metamaterials for broadband absorption with high melting temperature are attracting researchers' interests because of the applications working with high temperature [43].

Among all of those metamaterials for broadband perfect absorption, those with cone-like nanostructures have been studied because of their easy to be fabrication and the simple principle achieving broadband absorption. Ken et al. proposed the first prototype of such kind of absorber to enhance the solar energy conversion by Si for solar cell in the wavelength range of 300–1000 nm [44]. Then, some more studies have been carried out to design the absorbers with nearly perfect absorption band [45–47]. The reflection suppression effect from a three-dimensional structure with increasing cross-section along the direction of incident light dominates the broadband absorption of light for such kind of absorbers. However, most of those previous absorbers made of cone-like structures merely showed perfect absorption for solar energy harvesting. In the present study, the absorber based on tapered nanostructures, which have a drastically varying cross-sectional area in the axial direction along the incident light will be numerically studied and optimized for perfect absorption of

solar energy. The optimization will be carried out with the materials, geometric parameters, as well as morphologies of the cones. The incident angle and polarization of the light source are also taken into consideration. The finite difference time domain (FDTD) method based on Maxwell's equations is used on optimization of these parameters for perfect absorption of solar energy [48,49].

2. Model description

The three-dimensional (3D) calculated model of the proposed absorber is shown in Figure 1(a), and a basic unit structure with various geometric parameters is shown in Figure 1(b), while Figure 1(c) illustrates nanocones covered by a layer made of another material. As shown in Figure 1, the proposed structure consists of a substrate, a gold layer on the substrate, and an array of nanocones on the top with a Al_2O_3 dielectric layer in-between. The Au layer has a high reflectivity, so the light transmitted through Al_2O_3 layer can be reflected back to the upper nanostructure to be absorbed again. A Al_2O_3 layer forms metal-insulator-metal [50] (MIM) structure with the upper and bottom layers, which can improve the absorption effect of the absorber. The top nanocones are made of different materials with different geometric parameters for the optimization. The nanocones are regularly arranged on the top of the proposed absorber, the distances between the two units in the *x* and *y* directions are both *l*, and the whole structure looks like a square matrix. The height of the nanocones is denoted by *h* and the diameter of their bottom circle is represented by *D*, the nanocones in FDTD calculations are infinitely sharp, in other words, the radius at the top is 0. The thickness of the Al_2O_3 layer and Au layer is respectively represented by *a* and *b*, while the thickness of the SiO_2 substrate is *c*, and the SiO_2 substrate is used to sustain the whole structure, which can be removed during the calculation of the absorber's optical properties.

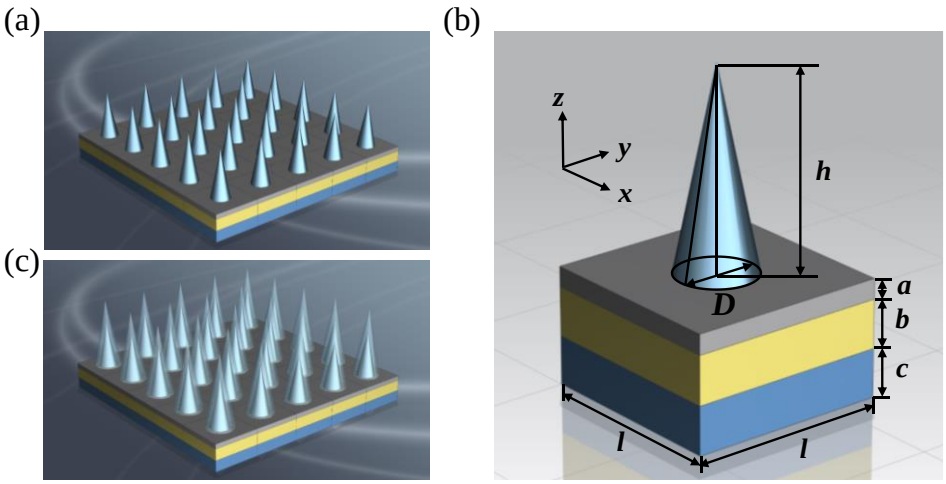

Figure 1. The schematic of the proposed absorber. (a) 3D schematic of the absorber with regularly arranged nanocone array. The bottom blue region is a SiO_2 substrate, the up gray region is made of Al_2O_3, and the in-between yellow layer is made of Au. (b) A basic unit of the absorber with geometric parameters marked as follows: height of the nanocones (*h*), diameter of the nanocones (*D*), thickness of the Al_2O_3 layer (*a*), thickness of the Au layer (*b*), thickness of the substrate (*c*), size of the unit (*l*). (c) 3D schematic of the absorber with nanocones made of Si covered by a Cr layer.

In the present study, the refractive index of the Al_2O_3 is 1.75 in the interested spectral range, and the surrounding medium around the metamaterial is water with a refractive index of 1.33, and there will be minor change in absorptance when water is replaced by air (Figure S1). All the other dielectric functions of the used materials are taken from those data compiled by Palik [51] except for Bi_2Te_3 from Esslinger et al. [52]. It should be noted that in order to better fit the refractive index of all the materials in the present study to lower calculation errors, the wavelength region is divided into two or more parts. For example, the dielectric function of Cr is divided into two sections for the calculation, which are 300–1400 nm and 1400–2400 nm, respectively. The light source is a plane wave with the wavelength range of 300–2400 nm, which occupies most of the solar radiation spectrum on earth, and the initial direction of the incident light source is the negative *z* direction. In the numerical simulation, the periodic boundary conditions are used in the *x* and *y* directions according to the periodicity of the nanocones' arrangement, while the boundary condition in the *z* direction is perfectly matched layer (PML).

Based on the Maxwell equations and FDTD method, the reflectance (*R*) and transmittance (*T*) of the proposed absorber can be calculated by the commercial software FDTD Solutions. Then, the absorptance (*A*) of the absorber can be calculated by the formula of $A = 1-R-T$. Based on the formula for the calculation of *A*, it can be seen that the reduction of reflectance and transmittance of the absorber is the only way to increase the absorptance of it. For absorbers with multiple layers of materials, it is easy to achieve zero transmittance by selecting the appropriate bottom layer material with a thickness larger than 100 nm, which can be calculated by $\lambda/4\pi k$ with λ and k are the wavelength of the light and extinction coefficient of the material at the same wavelength. However, it is usually difficult to reduce the reflectance to a very low level, so we mainly focus on the reduction of the absorber's reflectance in the present study. When a cone-like nanostructure being submerged in water, the mixture of water and nanostructures can be regarded as an effective homogeneous medium, whose effective dielectric function (ε_{eff}) of each layer can be calculated as follows (TM electromagnetic wave) [53,54],

$$\frac{1}{\varepsilon_{\text{eff}}} = \frac{f}{\varepsilon_{\text{cone}}} + \frac{1-f}{\varepsilon_{\text{water}}} \tag{1}$$

where $\varepsilon_{\text{cone}}$ and $\varepsilon_{\text{water}}$ are dielectric functions of materials for cone and water respectively. f (a function of h) is the surface filling factor of nanocones at each cross section, which can be calculated by the ratio of cross section of the nanocone and the area of the periodic domain l^2. For the optical absorber with nanocones, the cross sectional area along the negative *z* direction (Figure 1(b)) is increasing. It can be found from Eq 1 that ε_{eff} increases from $\varepsilon_{\text{water}}$ to around $\varepsilon_{\text{cone}}$ from the top of nanocones to the bottom of them with the value of f increasing from 0 to the maximum in the negative *z* direction. The effective refractive index (n) and extinction coefficients (k) can be obtained from the effective dielectric function (Eq 1) as follows [53],

$$\varepsilon_{\text{eff}} = (n_{\text{eff}} + ik_{\text{eff}})^2 \tag{2}$$

It is found from Eqs 1 and 2 that the effective refractive index n_{eff} of the proposed absorber with nanocones on the top gradually increases in the negative *z*-direction (Figure 1b) from 1.33 of water to a larger value for material of nanocones with the increasing cross section of the nanocones in the same direction. The gradient increasing refractive index twists the light of any incident angle to nearly vertical direction at the bottom of the nanocones, while it is impossible for the unabsorbed

light reflects back to the surrounding medium. As one of the types of reflection suppression effect, gradient index effect will suppress the reflection of the incident light at the bottom of the nanocones to enhance the absorption property of the absorbers with nanocones on the top. However, it should be pointed outed that effective medium theory is valid only when the wavelength of the light is much longer than the nanostructures period, meaning that not all the cases considered in the present study satisfy such a theory. Therefore, the effective refractive index effect and gradient index effect will be used to provides certain qualitative insights for the optimization of the absorbers with cone-like structures in the present study, and rigorous numerical solutions on field and dissipation distributions for the interaction of electromagnetic waves with nanostructures are obtained.

3. Results and discussion

Absorption spectra of three different absorbers after the optimization are shown in Figure 2(a). Those three absorbers exhibit perfect absorption for solar energy with the following parameters: h = 2000 nm, h_0 = 1600 nm, D = 400 nm, d = 320 nm, l = 400 nm, a = 12 nm, and b = 100 nm. Our absorber is designed based on metal-insulation-metal (MIM) structure with Al_2O_3 acting as the insulating layer. A Au layer works as the reflective layer, and a SiO_2 substrate layer support the whole structure without absorbing the incident light, which can be removed in the calculation.

The mechanisms of perfect solar energy absorption of nanocones made of Bi_2Te_3 can be explained by gradient index effect and slow-light effect in our previous work [39]. It should be noted that the absorptance of an absorber with nanocones made of Si covered by a Cr layer (black solid line) is higher than 0.977 in the whole wavelength range of 300–2400 nm, which is slightly lower than the absorbance of the absorber using Cr nanocone in long wavelength range, but higher in the short wavelength range. The results demonstrate that the present absorber can be manufactured by covering one thin special layer on those nanocones made of materials easily to be fabricated by traditional nano-fabrication methods, which greatly lower the challenge of the fabrication process of such kind of perfect absorbers with nanocones.

For the optical absorber with nanocones, the cross sectional area along the negative z direction (Figure 1(b)) is increasing. It can be found from Eqs 1 and 2 that n_{eff} increases along the negative z direction with f increasing from 0 to the maximum in the same direction. The gradient increasing refractive index twists the light of any incident angle to nearly vertical direction at the bottom of the nanocones, while it is impossible for the unabsorbed light reflects back to the surrounding medium. The gradient index effect will suppress the reflection of the incident light at the bottom of the nanocones to enhance the absorptance of the absorbers with nanocones on the top. The electric fields in x-z plane are shown in Figure 2(b-II) and (c-II) for nanocones made of Cr and Si covered by a Cr layer, respectively. It can be found that there is high electric field at the bottom of the nanocones, indicating that the gradient index effect suppresses the light at the bottom of nanocones for not escaping from the proposed absorber.

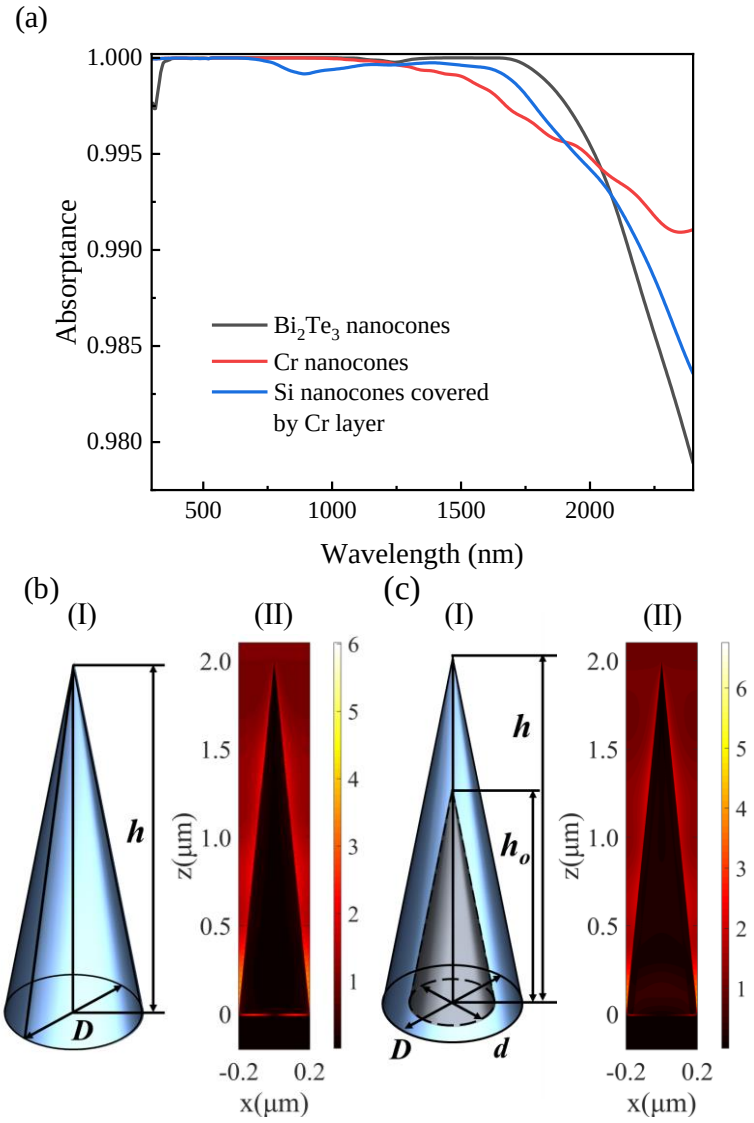

Figure 2. Absorption properties of three proposed absorbers. (a) The absorptance of the absorbers, the nanocones are respectively made of Bi_2Te_3, Cr and Si covered by a Cr layer. (b,c) The electric field distributions of absorbers with nanocones made of Cr and Si covered by a Cr layer, respectively. In each figure, (I) The morphology of the nanocones, (II) the electric field in *x*-*z* plane. Geometric parameters are h = 2000 nm, h_0 = 1600 nm, D = 400 nm, d = 320 nm, l = 400 nm, a = 12 nm, and b = 100 nm.

Figure 3 demonstrates the parameters affect the absorption properties of the proposed absorber with nanocones, and parameters are set as follows otherwise if indicated: h = 2000 nm, D = 400 nm, l = 400 nm, a = 12 nm, and b = 100 nm. As shown in Figure 3(a), these absorbers with nanocones made of Ag, Al, Au and Cu have a perfect absorption to the incident light in the short wavelength region of 300–650 nm because these materials have a large imaginary part of the dielectric function in the same region. However, the imaginary parts of the dielectric function of these four materials drastically decrease afterwards, leading to a fact that the absorptance of absorbers with nanocones made of these four materials decreases a lot afterwards. In contrast, the imaginary parts of the dielectric

functions of Cr, Ni, Pt as well as Ti are very large in the whole wavelength range of 300–1400 nm, the absorptance of absorbers made of these four materials demonstrates almost perfect solar energy absorption. The results demonstrate that the strong intrinsic absorption property of the materials for nanocones guarantees the broadband absorption of the proposed absorber for totally solar energy harvesting.

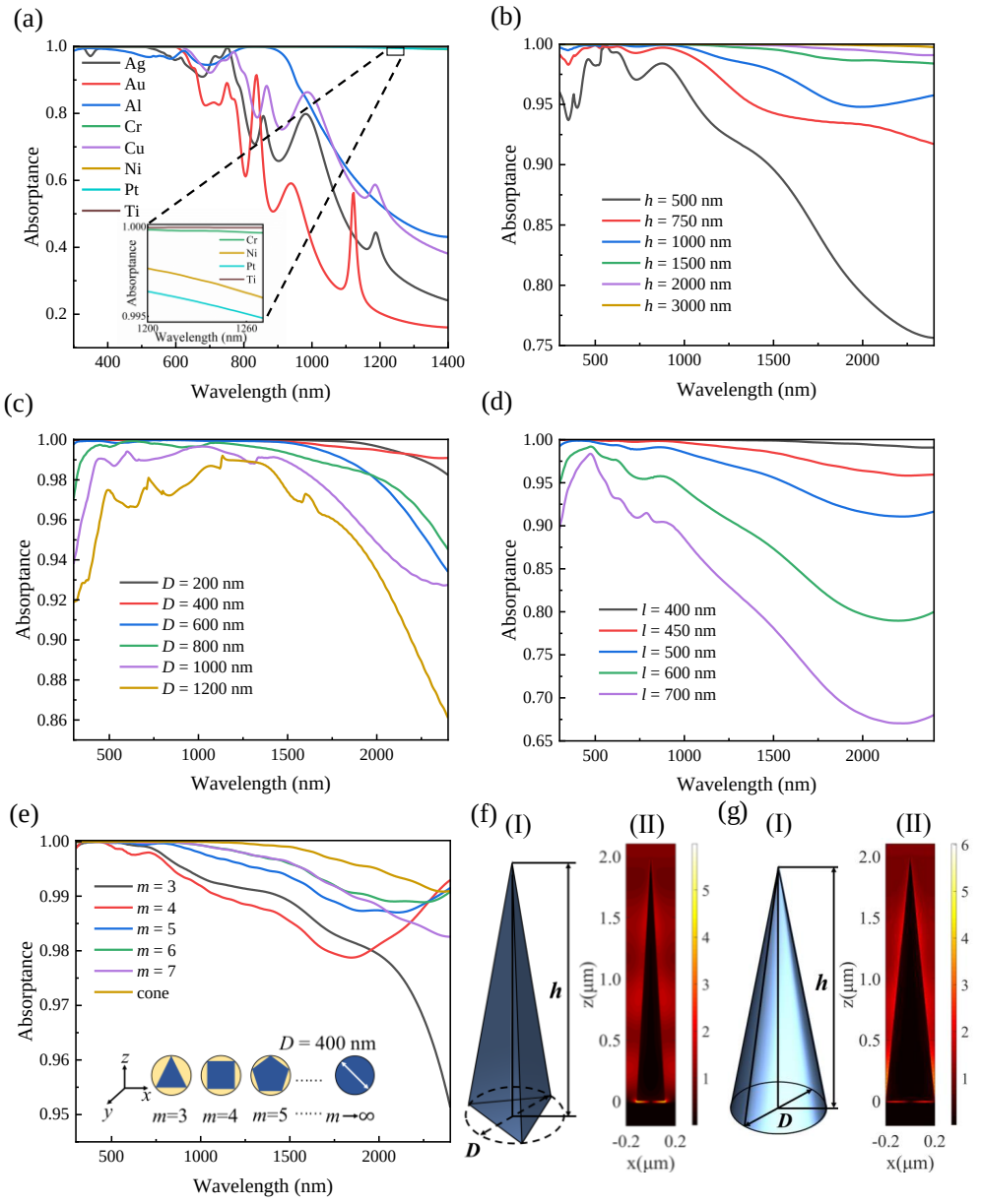

Figure 3. Parameters affect absorption spectra of absorbers. (a) The effect of materials. (b) The effect of the height of Cr nanocone. (c) The effect of the diameter of the Cr nanocone. (d) The effect of the distance between two adjacent Cr nanocones. (e) The morphologies of different Cr nanocones. (f,g) The electric field distributions of nanocones with different morphologies, (f) triangular cone, (g) circular cone. In each figure, (I) The morphology of the nanocones, (II) the electric field in *x*-*z* plane. h = 2000 nm, D = 400 nm, l = 400 nm, a = 12 nm, and b = 100 nm, otherwise if indicated.

The effects of geometric parameters of the nanocones made of Cr on the absorption properties are numerically studied (Figure 3(b)–(d)). All the nanocones with different heights (Figure 3(b)) exhibit excellent absorption property in the wavelength range of 300 nm to around 1300 nm, but there is a slight drop in the wavelength range of 1300 nm to 2400 nm. When the *h* reaches 2000 nm, the absorptance is greater than 99.1% in the entire wavelength range of 300–2400 nm. Figure 3(c) shows the effect of diameter of the nanocone on the absorption properties of the absorber for solar energy harvesting. When the diameter of the absorber changes in the range of 200–400 nm, the absorber has the best absorption effect. The absorptance of the absorber decreases with the increase of the diameter of the nanocone. It can be concluded that the diameter of the nanocones should be chosen carefully to meet the requirements of the gradient index effect of the absorber. The effect of the distance between two adjacent Cr nanocones is shown in Figure 3(d). The absorptance of the proposed absorber decreases with the increase of the distance between two nanocones, and the maximum absorptance of an absorber appears only if the distance between two nanocones is the same with the diameter of them. The underlying mechanisms are that the effective refractive index of the absorber at the top of nanocones is water for all the absorbers studied in Figure 3(d). However, the effective refractive indices at the bottom of the nanocones are totally different for different *l*. The larger of the *l*, the smaller of the effective refractive index of the absorber at the bottom of the nanocones, while a smaller refractive index at the bottom of nanocones significantly weakens the gradient index effect.

Some more morphologies of cone-like nanostructures are taken into consideration to further study the absorption properties of absorbers with cone-like nanostructures. The bottom circumscribed circles of these cone-like structures are the same, which is 400 nm. The number of sides of these regular polygon is represented by *m*, as shown in inset of Figure 3(e). The absorptance of all these absorbers is higher than 95%, and the absorber with circular nanocones has the best absorption property in the wide solar spectrum. In contrast, the absorptance of an absorber with triangular nanocones is the lowest among all the proposed absorbers. The underlying mechanisms are revealed by the electric field distributions for triangular nanocones (Figure 3(f-II)) and circular nanocones (Figure 3(g-II)) at the wavelength of 1800 nm. The electric fields in *x*-*z* plane between two circular nanocones is the lower one, while the electric field at the top of circular nanocones is the weaker one. The cross sectional area of the circular nanocone is the largest at the same attitude for these cone-like structures, including at the bottom of the nanocone, leading to a fact that the effective refractive index of circular nanocone is the largest (based on Eqs 1 and 2) among all the six different cone-like structures. The difference of the effective refractive indices at the top and the bottom increases with the increase of *m*, the magnitude of the electric field at the bottom of nanocones increases with the increase of *m*, leading to a fact that the absorptance of the absorber also increases with the increase of *m* (Figure 3(e)).

With the rotation and revolution of the earth, the incident angle of the sunlight will change for a fixed absorber. It can be found from Figure 4(a) that the absorptance of the absorber reaches the maximum in the entire broad solar spectrum if the light normally incidents on the absorber, while the absorptance of the absorber decreases with the increase of the incident angle. The reason is that the light source only illuminates the part facing it when the incident angle of the light source is tilted, and the backlight surface cannot absorb the light and reflect it back to the surrounding medium, resulting in the decrease of the absorptance of the absorber.

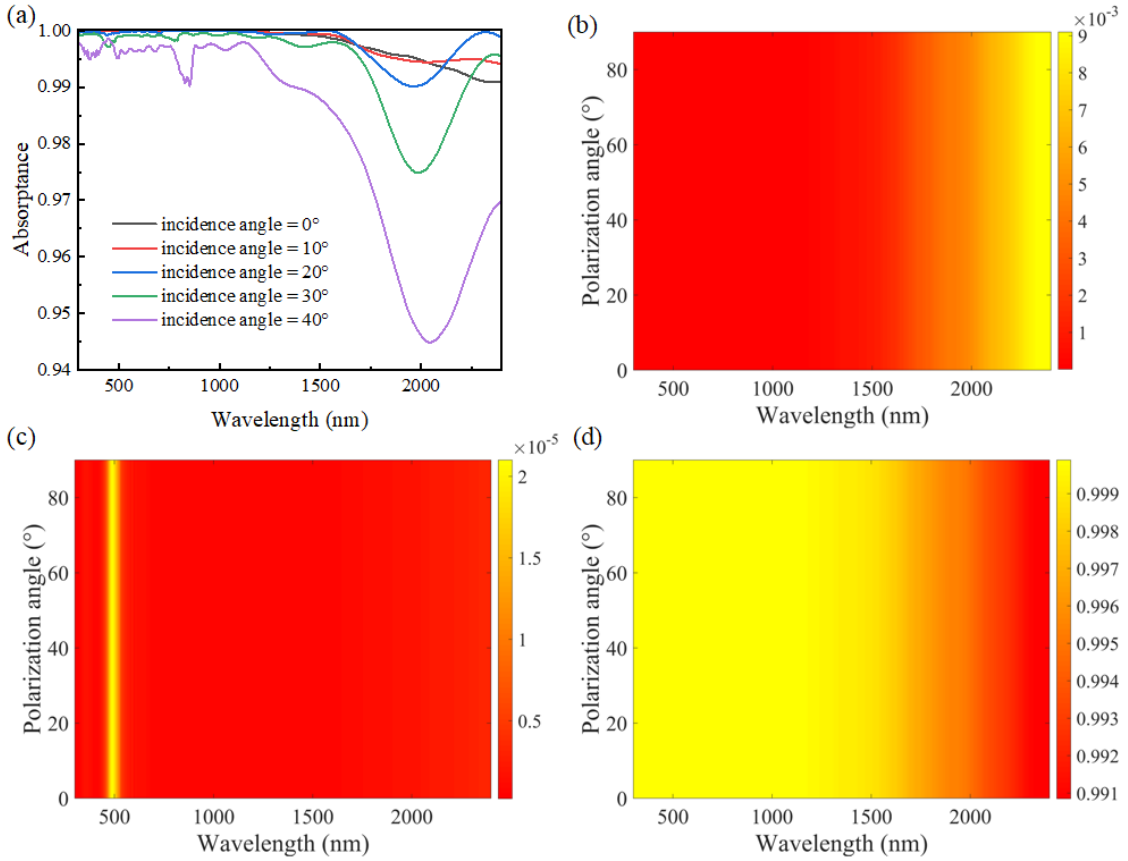

Figure 4. The effects of incident angle and polarization of light on the absorptance of the proposed absorbers, h = 2000 nm, D = 400 nm, l = 400 nm, a = 12 nm, and b = 100 nm. (a) The absorption spectra for different incident angles. (b–d) The effect of polarization of the incident light on the absorption properties ((b) reflectance, (c) transmittance, (d) absorptance) of the present absorbers with Cr nanocones.

The polarization phenomenon of the light source reveals the asymmetry of the vibration direction of light with respect to the propagation direction of light. It can be observed from Figure 4(b)–(d) that the reflectance and transmittance of absorbers with Cr nanocones are very low with the polarization of the incident light varies in the range of 0–90º, and the absorptance is higher than 99.1% for all the polarization angles of the incident light. As shown in Figure 1, the nanocones are rotationally symmetrical with the centerline. Therefore, for a light source of a fixed wavelength, the change of the polarization angle almost makes no difference on the absorption property of an absorber with Cr nanocones on the top. But for some other absorbers with pyramids shown in Figure 3(e), the polarization angle might make a difference on the absorption properties of those absorbers.

4. Conclusions

In summary, we have numerically studied the effects of materials, geometric parameters, morphologies, incident angles and polarization of the light source on the absorption property of the absorber with nanocones surrounded by water to optimize the absorption of solar energy. The results

show that the optimized absorber has almost perfect absorption property in a wide wavelength range of 300–2400 nm, which is suitable for the total solar energy harvesting. Besides, the absorption property of the present absorber based on nanocones is independent of the polarization angle of the light source, but a small deviation of the incident angle significantly affects the absorptance of the absorber with Cr nanocones. Furthermore, the morphology and geometric parameters of the nanocones also make a big difference on the absorption properties of the proposed absorbers with a small tolerance. An absorber with circular nanocones made of Cr, Ni, Ti, Pt, and Bi_2Te_3, has the best absorption property for solar energy harvesting. The underlying mechanisms of the absorption properties of the present absorber are well revealed by the combination of effective refractive index theory and gradient index effect. The absorber is placed in water, which can accelerate the evaporation of water by absorbing light energy and converting it into heat energy, so our study opens a new gate for the design of absorbers for the conversion and utilization of solar energy in water.

Acknowledgements

This work was supported by National Natural Science Foundation of China through Grant No. 52006056 and by Natural Science Foundation of Hunan through Grant No. 2020JJ3012. The project was also supported in part by Science and Technology Bureau Foundation of Changsha City (kh1904005).

Conflict of interest

The authors declare no conflict of interest.

Supplementary

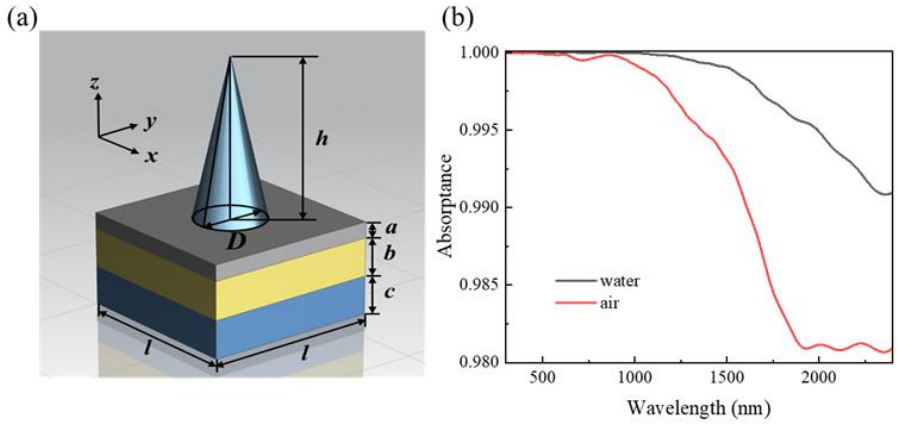

Figure S1. (a) A basic unit of the absorber with geometric parameters marked as follows, height of the nanocones (*h*), diameter of the nanocones (*D*), thickness of the Al_2O_3 layer (*a*), thickness of the Au layer (*b*), thickness of the substrate (*c*), size of the unit (*l*). (b) The absorptance of the absorbers, the surrounding media are water and air. Figure S1 (b) demonstrates the absorption property of the absorber in air is lower than that in water. However, the absorption property can be enhanced by adjusting the geometric parameters.

References

1. Linic S, Aslam U, Boerigter C, et al. (2015) Photochemical transformations on plasmonic metal nanoparticles. *Nat Mater* 14: 567–576.
2. Takashima T, Hikosaka K, Hirose T (2004) Photosynthesis or persistence: nitrogen allocation in leaves of evergreen and deciduous Quercus species. *Plant Cell Environ* 27: 1047–1054.
3. O'regan B, Grätzel M (1991) A low-cost, high-efficiency solar cell based on dye-sensitized colloidal TiO_2 films. *Nature* 353: 737–740.
4. Chen CJ, Kuang YD, Hu LB (2019) Challenges and opportunities for solar evaporation. *Joule* 3: 638–718.
5. Solangi KH, Badarudin A, Aman MM, et al. (2015) Photochemical transformations on plasmonic metal nanoparticles. *Renew Sust Energy Rev* 41: 1190–1204.
6. Wolf M (1974) Solar energy utilization by physical methods. *Science* 184: 382–386.
7. Qasuria TA, Alam S, Karimov KS, et al. (2019) Stable perovskite based photodetector in impedance and capacitance mode. *Results Phys* 15: 102699.
8. Qasuria TA, Fatima N, Karimov KS, et al. (2020) A novel and stable ultraviolet and infrared intensity sensor in impedance/capacitance modes fabricated from degraded CH3NH3PbI3-Cl-x(x) perovskite materials. *J Mater Res Technol* 9: 12795–12803.
9. Yang P, Liu K, Chen Q, et al. (2017) Solar-driven simultaneous steam production and electricity generation from salinity. *Energy Environ Sci* 10: 1923–1927.
10. Neumann O, Feronti C, Neumann AD, et al. (2013) Compact solar autoclave based on steam generation using broadband light-harvesting nanoparticles. *Proc Natl Acad Sci* 110: 11677–11681.
11. Lenert A, Bierman DM, Nam Y, et al. (2014) A nanophotonic solar thermophotovoltaic device. *Nat Nanotechnol* 9: 126–130.
12. Boghossian AA, Ham MH, Choi JH, et al. (2011) Biomimetic strategies for solar energy conversion: a technical perspective. *Energy Environ Sci* 4: 3834–3843
13. Cavusoglu AH, Chen X, Gentine P, et al. (2017) Potential for natural evaporation as a reliable renewable energy resource. *Nat Commun* 8: 1–9.
14. Lewis NS (2016) Research opportunities to advance solar energy utilization. *Scinece* 351: aad1920.
15. Oki T, Shinjiro K (2006) Global hydrological cycles and world water resources. *Science* 313: 1068–1072.
16. Hao J, Zhou L, Qiu M (2011) Nearly total absorption of light and heat generation by plasmonic metamaterials. *Phys Rev B* 83: 105107.
17. Watts CM, Liu X, Padilla WJ (2012) Metamaterial electromagnetic wave absorbers. *Adv Mater* 24: OP98–OP120.
18. Landy NI, Sajuyigbe S, Mock JJ, et al. (2008) A perfect metamaterial absorber. *Phys Rev Lett* 100: 207402.
19. Ni GW, Li G, Boriskina SV, et al. (2016) Steam generation under one sun enabled by a floating structure with thermal concentration. *Nat Energy* 1: 1–7.
20. Neumann O, Urban AS, Day J, et al. (2013) Solar vapor generation enabled by nanoparticles. *ACS Nano* 7: 42–49.

21. Fang ZY, Zhen YR, Neumann O, et al. (2013) Evolution of light-induced vapor generation at a liquid-immersed metallic nanoparticle. *Nano Lett* 13: 1736–1742.
22. Zhu MW, Li YJ, Chen FJ, et al. (2018) Plasmonic wood for high-efficiency solar steam generation. *Adv Energy Mater* 8: 1701028.
23. Chen MJ, He YR, Huang J, et al. (2016) Synthesis and solar photo-thermal conversion of Au, Ag, and Au-Ag blended plasmonic nanoparticles. *Energy Convers Manage* 127: 293–300.
24. Richardson HH, Carlson MT, Tandler PJ, et al. (2009) Experimental and theoretical studies of light-to-heat conversion and collective heating effects in metal nanoparticle solutions. *Nano Lett* 9: 1139–1146.
25. Baffou G, Girard C, Quidant R (2010) Mapping heat origin in plasmonic structures. *Phys Rev Lett* 104: 136805.
26. Cao L, Barsic DN, Guichard AR, et al. (2007) Plasmon-assisted local temperature control to pattern individual semiconductor nanowires and carbon nanotubes. *Nano Lett* 7: 3523–3527.
27. Baffou G, Quidant R, Girard C (2009) Heat generation in plasmonic nanostructures: Influence of morphology. *Appl Phys Lett* 94: 153109.
28. Shi L, He YR, Wang XZ, et al. (2018) Recyclable photo-thermal conversion and purification systems via Fe_3O_4@TiO_2 nanoparticles. *Energy Convers Manage* 171: 272–278.
29. Hu Y, Wang RZ, Wang SG, et al. (2016) Multifunctional Fe_3O_4@Au core/shell nanostars: a unique platform for multimode imaging and photothermal therapy of tumors. *Sci Rep* 6: 1–12.
30. Wang J, Li YY, Deng L, et al. (2017) High-performance photothermal conversion of narrow-bandgap Ti_2O_3 nanoparticles. *Adv Mater* 29: 1603730.
31. Chen R, Wu ZJ, Zhang TQ, et al. (2017) Magnetically recyclable self-assembled thin films for highly efficient water evaporation by interfacial solar heating. *RSC Adv* 7: 19849–19855.
32. Vélez-Cordero JR, Hernández-Cordero J (2015) Heat generation and conduction in PDMS-carbon nanoparticle membranes irradiated with optical fibers. *Int J Therm Sci* 96: 12–22.
33. Shelby RA, Smith DR, Schultz S (2001) Experimental verification of a negative index of refraction. *Science* 292: 77–79.
34. Dutta HS, Goyal AK, Srivastava V, et al. (2016) Coupling light in photonic crystal waveguides: A review. *Phnotnic Nanostruct* 20: 41–58.
35. Smith DR (2004) Metamaterials and negative refractive index. *Science* 305: 788–792.
36. Ra'di Y, Asadchy VS, Kosulnikov SU, et al. (2015) Full light absorption in single arrays of spherical nanoparticles.
37. Monti M, Alù A, Toscano A, et al. (2019) The design of optical circuit-analog absorbers through electrically small nanoparticles. *Photonics* 6: 1–11.
38. Wang ZL, Zhang ZM, Quan XJ, et al. (2018) A perfect absorber design using a natural hyperbolic material for harvesting solar energy. *Sol Energy* 159: 329–336.
39. Tao P, Ni G, Song C (2018) Solar-driven interfacial evaporation. *Nat Energy* 3: 1031–1041.
40. Zhou L, Tan YL, Ji DX, et al. (2016) Self-assembly of highly efficient, broadband plasmonic absorbers for solar steam generation. *Sci Adv* 2: e1501227.
41. Zhao B, Zhang ZMM (2017) Perfect mid-infrared absorption by hybrid phonon-plasmon polaritons in hBN/metal-grating anisotropic structures. *Int J Heat Mass Transf* 106: 1025–1034.
42. Hu HF, Ji DX, Zeng X, et al. (2013) Rainbow trapping in hyperbolic metamaterial waveguide. *Sci Rep* 3: 1249.

43. Liang QQ, Yin Q, Chen L, et al. (2020) Perfect spectrally selective solar absorber with dielectric filled fishnet tungsten grating for solar energy harvesting. *Sol Energy Mat Sol C* 215: 110654.
44. Wang KXZ, Yu ZF, Liu V, et al. (2012) Absorption enhancement in ultrathin crystalline silicon solar cells with antireflection and light-trapping nanocone gratings. *Nano Lett* 12: 1616–1619.
45. Wang KXZ, Yu ZF, Liu V, et al. (2014) Nearly total solar absorption in ultrathin nanostructured iron oxide for efficient photoelectrochemical water splitting. *ACS Photonics* 1: 235–240.
46. Wang JX, Liang YZ, Huo PC, et al. (2017) Large-scale broadband absorber based on metallic tungsten nanocone structure. *Appl Phys Lett* 111: 251102.
47. Argyropoulos C, Le KQ, Mattiucci N, et al. (2013) Broadband absorbers and selective emitters based on plasmonic Brewster metasurfaces. *Phys Rev B* 87: 2051112
48. Maxwell JC (1864) A dynamical theory of the electromagnetic field, London: Royal Society.
49. Yee KS (1966) Numerical solution of initial boundary value problems involving maxwell's equations in isotropic media. *IEEE T Antennn Propag* 14: 302–307.
50. Feng P, Li WD, Zhang WH (2015) Dispersion engineering of plasmonic nanocomposite for ultrathin broadband optical absorber. *Opt Express* 23: 2328–2338.
51. Pailk ED (1985) Handbook of optical constants of solids, New York: Academic Press.
52. Esslinger M, Vogelgesang R, Talebi N, et al. (2014) Tetradymites as natural hyperbolic materials for the near-infrared to visible. *ACS Photonics* 1: 1285–1289.
53. Bohren CF, Huffman DR (1998) Absorption and scattering of light by small particles, New Jersey: Wiley.
54. Zhang ZM (2007) Nano/microscale heat transfer, New York: Springer.

AIMS Press